AN EXPERIMENTAL STUDY OF FREQUENCY DROOP CONTROL IN A LOW-INERTIA MICROGRID

BY

ANDREW MARK BOLLMAN

THESIS

Submitted in partial fulfillment of the requirements
for the degree of Master of Science in Electrical and Computer Engineering
in the Graduate College of the
University of Illinois at Urbana-Champaign, 2009

Urbana, Illinois

Adviser:

Professor Philip T. Krein

ABSTRACT

The use of distributed generation in microgrid systems is becoming a popular way to provide a reliable source of electricity to critical loads. Efforts in disaster relief operations and national defense applications require a mobile, scalable power grid that is easily constructed and robust enough to handle radical system changes. These microgrids are usually built using low-inertia generators that are portable and can easily adapt to a rapidly changing environment. Despite the benefits of low-inertia generation, the drawback is that large load steps can cause a system to become unstable, losing synchronism and damaging both generators and loads. A control system is necessary to bring stability while providing efficient and robust electricity to the microgrid.

A droop control scheme uses only local power to detect changes in the system and adjust the operating points of the generators accordingly. The droop control uses the real power out of a generator to calculate the ideal operating frequency. This relaxing of a stiff frequency allows the microgrid to dampen the fast effects of changing loads, increasing the stability of the system. Droop control is reviewed and simulations will be used to determine the effectiveness of the droop controller as well as alternative forms of the traditional droop control. Experimental results are presented detailing how the droop gain affects power distribution and system stability.

ACKNOWLEDGMENTS

I would like to thank my adviser Professor Philip T. Krein for the opportunity to study under his guidance. His guidance and advice has been much appreciated.

I would also acknowledge the U.S. Army Corps of Engineers Engineering Research and Development Center, Construction Engineering Research Laboratory (ERDC-CERL), for providing funding and encouragement to complete this work. Also, thank you to the many friends and family for keeping things in perspective the last few years.

TABLE OF CONTENTS

LIST OF FIGURES

LIST OF TABLES

1. BACKGROUND

A distributed generator is defined as an electric power source connected to the distribution network or directly at the customer application [1]. Due to the increasing load requirements on the electrical system and the high capital investment that large centralized power plants require, a study by the Electric Power Research Institute (EPRI) indicates that by 2010, 25% of the new generation will be distributed [2]. The high penetration of distributed generation units in the electrical system can significantly impact the flow of power and voltage conditions at the end customers [3]. A microgrid can create a small robust system utilizing many of these distributed generation units by using local information at each generator. Microgrids offer many advantages over the traditional centralized electrical system [4, 5]. The focus of this work is on the power reliability that distributed generation coupled with a microgrid concept can achieve.

1.1 Applications of Distributed Generation

There are many applications that require a high level of reliability and robustness in the electrical infrastructure. Traditional applications include back-up power devices for the telecommunications industry but the concept can be expanded to disaster relief efforts, national defense applications and anytime there is a lack of a central electrical infrastructure. While a telecommunications network has a never-fail requirement, other applications may have different objectives and unique challenges. Response time is short for disaster relief efforts and very little site engineering can be done in advance of setting up an electrical distribution network. The ability to create a power system that can be easily changed with little engineering would provide the flexibility to add generators and

loads as the relief effort evolved. At the same time, this system should also provide energy to critical structures such as field hospitals and communication centers.

Department of Defense applications have another set of unique challenges that require an adaptable, robust and reliable electrical network. A large military installation is like a city unto itself containing shopping centers, movie theaters and living quarters for tens of thousands of people. Often such an installation has a small number of feeder lines that provide all the electrical power to the base. This creates a security issue since the installation's mission can be severely compromised if the power supply from one of the feeder lines is interrupted for natural or unnatural reasons. It would be desirable if these installations had an adaptable power system that would detect instability in the system while utilizing a controller that would help the system absorb and dampen the effects of the disturbances avoiding a total system collapse. Coupled with priority-based load shedding and intelligent power sharing, such a system would insure that power is delivered to critical loads and while keeping the installation at a high state of readiness.

1.2 Microgrid Concept

It has been proposed that one solution to the reliability and stability issues is to take advantage of microgrid technologies. The term "microgrid" is quickly becoming a popular topic within the power community but it still remains vaguely defined. For the purposes of this work, a microgrid is defined as a *subsystem of distributed energy sources and their associated loads* [6]. This approach allows for the local control of the distributed generation, thereby reducing or eliminating the need of a central controller. A

microgrid can be a stand-alone system or it can be tied to a stiff ac grid that it separates from during disturbances.

A microgrid offers three major advantages over a traditional electricity supply involving central generation stations, long distance energy transmission over a network of high voltage lines, then distribution through medium voltage networks [4]:

- Application of combined heat and power technology
- Opportunities to tailor the quality of power delivered to suit the requirements of end users
- Create a more favorable environment for energy efficiency and small-scale renewable generation investments

The use of waste heat through co-generation or combined heat and power processes (CHP) implies an integrated energy system, delivering both electricity and useful heat from an energy source. Combined heat and power processes can convert as much as 90 percent of its fuel into useable energy [7]. To maximize the efficiency of the unit, the sources need to be placed close to the heat load rather than the electrical load since it is easier to transport electricity over longer distances. Small local sources can be sited optimally for heat utilization, so that a distributed system that is integrated with distributed generation is very pro-CHP.

Power quality and power reliability are often used in quantifying levels of electrical service [8]. Both scheduled and unscheduled outages affect the availability of certain services and processes to the end-users as well as increasing dependence on on-site

backup generation which can be costly. The deterioration in power quality has more subtle, but important, effects as well. Voltage sags, harmonics and imbalances are triggered by switching events or faults in the electrical system. While power quality events do not lead to electrical loss, they can degrade the power in the end-use processes, affecting equipment performance and durability. Distributed energy sources have the potential to increase system reliability and power quality due to the decentralization of supply. Increase in reliability levels can be obtained if distributed generation is allowed to operate autonomously in transient conditions, mainly if there is an outage or disturbances upstream in the electrical supply.

The integration of renewable energy sources into the power system provides unique challenges to the designers of the electrical system. Due to the intermittent nature of the sources, central generation is required to provide the base power supply as well as provide backup power when the sun is not shining or the wind is not blowing. Systems with intermittent sources can experience similar problems as systems with large, intermittent loads. Distributed generation can ease the burden of high penetration of renewable sources by filling in when intermittent generation is low and by smoothing the transmission system loading.

Many studies of renewable sources tie to the electrical system through inverters, which lack the mechanical inertia that helps bring stability to the grid. There are different inverter topologies that inherently have electrical storage on the output, such as voltage-sourced inverters, replicating the energy stored in a rotating machine, and this lends them

well for microgrids [9]. Much of the previous work on the integration of renewable energy into microgrids focuses on the control of the inverter that ties the source to the electrical system.

1.3 Microgrid Architecture

A traditional architecture of a microgrid is shown in Figure 1 with a microgrid connected to a larger system and a disconnect switch that "islands" the distributed generation units to protect sensitive loads. A major factor in microgrids is the creation of the disconnect switch that will enable the microgrid to maintain compliance with current commercial standards such as IEEE 1547 [10]. Such a switch is necessary to realize the high reliability and power quality that microgrids offer.

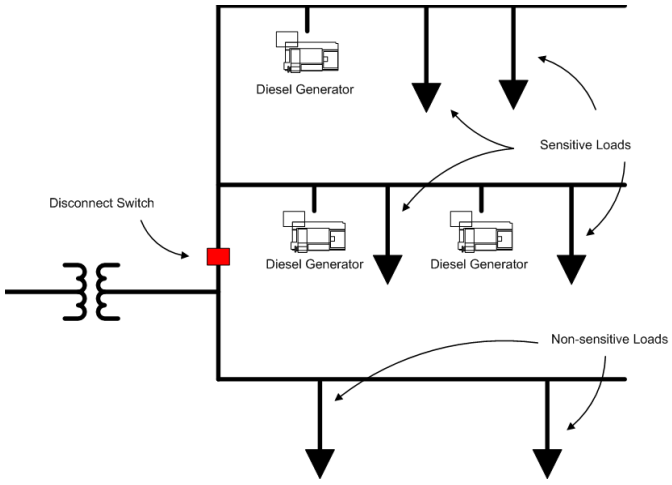

Figure 1. Microgrid Architecture

It has been found that in terms of energy security, multiple small generators are more efficient than relying on a single large generator [11]. Small generators have a lower inertia and are better at automatic load following and help avoid large standby charges that occur when there is only a single large generator. Having multiple distributed

generators available makes the chance of an all-out failure less likely, especially if there is backup generation capable of being quickly and easily connected to the system.

This configuration of multiple independent generators creates a peer-to-peer network that insures that there is no master controller that is critical to the operation of the microgrid. Having a component such as a master controller creates a single point of failure which is not the ideal situation when the end user demands high reliability in the electrical system. A peer-to-peer system implies that the microgrid can continue to operate with the loss of any component or generator. With the loss of one source, the grid should regain all its original functionality with the addition of a new source, if one is available. This ability to interchange generators and create components with plug-and-play functionality is one requirement of microgrids.

Plug-and-play elements imply not only that any unit is replaceable but that a unit can be placed at any point in the system without re-engineering the controls. This functionality of plug-and-play gives the benefit of placing generation close to the load, further increasing efficiency by reducing transmission losses. The concept can be extended to allowing generators to sit idly on the system when there is more electrical capacity than necessary. As the load on the system increases, additional generators would come online at a pre-determined set-point necessary to maintain the correct power balance. The set-point could use voltage sag, frequency droop or any other factor that indicates the system is being stressed to signal an increase in generator capacity. Intelligent devices could sense when there is extra generation capacity on the system and would disconnect and

turn off generators to save fuel and increase machine efficiencies. A scheme that would allow for generators to automatically drop off the system when there is no longer a high demand of power would assume a hierarchy of generators with different set-points so that not all the generators drop off at the same time.

1.4 Control Methods for Distributed Generation within a Microgrid

The lack of a master controller implies that autonomous controls will be necessary for both a peer-to-peer network and plug-and-play functionality. In addition to the increased network capabilities and functionality, if the distributed energy sources are allowed to operate autonomously in transient conditions, the reliability of the system increases [8]. If the load is suddenly increased or the system experiences the loss of a generator, the electrical sources will have the capability to take local data such as power voltage, power and frequency and create a new operating set-point that will insure stability in the system.

Grid-tied microgrids can be operated in three different configurations [12]. The first is the unit power control configuration where each distributed energy source regulates the voltage magnitude at the connection point and the power that the source is injecting. In this configuration, any change in load within the microgrid is provided power through the grid since every unit regulates to constant output power. This configuration is ideal for CHP applications because power production depends on heat demand. The second configuration is the feeder flow control configuration where each distributed generator regulates the voltage magnitude at the connection point and the power that is flowing into the microgrid. Extra load demands are picked up by the distributed energy sources and

so the microgrid looks like a constant load to the utility grid. With this configuration the microgrid becomes a dispatchable load as seen from the utility side, allowing for demand-side management. The third configuration is a hybrid of the previous two with some of the sources regulating their output power while others regulate the power into the microgrid. This configuration can have some units operating at peak efficiency utilizing waste heat, and other units ensuring that the power flow from the grid stays constant under changing load conditions.

1.5 Previous Works Involving the Control of Microgrids

Previous studies on the use of droop control within the context of controlling distributed generation focus on the idea that inverters will tie the energy source into the electrical system. Studies on control schemes for power balance, fault tolerance and system stability have been conducted but focus on the control of the power electronics topology and switching schemes to obtain results. These earlier works provide insight into droop control and some important studies are highlighted below.

Reference [13] discusses control of parallel operation multi-converters in a distributed generator system. The paper studies a distributed system with two distributed generation subsystems. In each subsystem there are two voltage source inverters and two loads. The controller uses an inner loop that regulates the current and an outer loop that controls voltage. A droop control calculates a reference voltage and compares that operating point with the current operating conditions creating an error signal. The error signals are then used by the controller to adjust the PWM signal for driving a full-bridge inverter. The

two sources in each subsystem operate in a master-slave relationship where the master sets the bus voltage and the slave controller achieves load sharing and power balance. As discussed in previous sections, a master-slave configuration creates a greater chance for failure, and the loops in the control law are unique to specific inverters, making the configuration difficult to use as a universal controller in a microgrid with multiple energy sources.

The widespread use of inverters providing power to a microgrid system can create higher-order harmonics due to internal switching. A hybrid approach is introduced in [14] that proposes inverters in close proximity operate in a master-slave relationship and load sharing between distant groups using frequency droop. The master inverter uses repetitive voltage control at the common node to suppress harmonic distortion and slave inverters use repetitive control in current mode. The paper proposes to modify the droop characteristic such that generation is increased at nodes with a large local load so that power exchanges through the distribution system are reduced from those that would occur in conventional droop schemes. Simulation results show that this hybrid control configuration can improve waveform quality by reducing the total harmonic distortion; however, the existence of the master-slave relationship and complexity of the voltage controller would create a controller specific to an application.

A voltage and frequency droop control scheme for parallel inverters is discussed that can be used to connect distributed energy sources to a microgrid, allowing both islanded mode operation and grid-connected operation. The droop equations are implemented by

controlling a power electronic inverter in order to behave like a voltage source with virtual resistive-inductive output impedance. The design of the controller is done using a linear quadratic Gaussian control structure which consists of a Kalman state observer and a control law [15]. The droop control is used to create references for the voltage and frequency which are compared to actual values to create an error signal. This signal is then used in the observer and control law to bring the inverter to the desired operating point. This controller introduces more complexity than the simple droop equation and any controller that includes an observer can create steady-state errors without exact parameter measurements. The reference discusses experimental results implementing the control scheme using an FPGA to generate the switching signals for the inverter and PC's monitor data and create the droop control. The energy source for the inverter is listed as a dc power supply and the experiments verified three phase operation of the control in both islanded mode and grid-connected mode.

Reference [16] proposes a voltage-power droop/frequency-reactive power boost control scheme, which allows current controlled voltage source converters (VSC) to operate in parallel on the same microgrid. Each VSC in the microgrid has its own controller that sets its current references to regulate the voltage and frequency of a common microgrid bus to track the drooped references. The control scheme provides voltage and frequency regulation of the microgrid in islanded mode, provides over-current protection of the VSC and requires only a single three-phase inductor in the VSC output interface. The controller included multiple PI loops and a transformation into the *d-q* reference frame.

Experiments by the paper's authors validated the joint control of the voltage and real and reactive power sharing using a dc power supply as the input for the inverters.

An analysis of a transient droop control that uses the droop method of real power-voltage and reactive power-frequency droop is given in [17]. The reactive power-frequency droop has a droop gain with a positive slope; the authors remark that if rotating-machine generator acting in accordance with conventional droop is connected to a converter system with the sources operating according to this transient droop method, the system becomes unstable. The study treats current control, frequency estimation and droop control for the converters of a distributed system consisting of an inverter source and rotating machines connected to a stiff grid. Matlab is used to find suitable controller and filter parameters from the small-signal analysis. A simulation of the full system is conducted in Dymola in order to verify the controller parameters as well as to compare the dynamic properties of the two droop methods. An experiment is conducted by the authors as well, but leaves out the rotating machine and external ac network. Their results show that power quality, load-sharing and dynamic properties are not affected by line impedances and that the sources operated satisfactorily with the new droop method.

Control of inverters in a stand-alone system is explored using a space vector PWM algorithm. The advantage of using a voltage vector is that the magnitude of the fundamental voltage can control the reactive power and the angle of the vector can be used to monitor the frequency of the inverter output [18]. The voltage vector can be obtained from local information, eliminating the need for a communication signal

between sources. One potential issue is that this scheme assumes a stiff frequency, limiting the range of applications in which it can be used.

Faults and load imbalances are a reality within any electrical distribution system and systems comprised of distributed generators are no exception. There is a need for a controller to help maintain stability, and [19] presents a control scheme for inverters to maintain a regulated output voltage in the presence of voltage imbalances resulting from system faults or load imbalances. The controller maintains voltage within the sensitivity levels of the equipment while the generators are in islanded mode, and it provides real and reactive power-flow control when operating in grid-tied mode. The controller uses multiple loops containing regulators for filter inductor current, filter capacitor voltage and real and reactive powers. Simulation results are shown in the study, verifying that the controller worked in both the grid-tied and islanded mode. Frequency regulation was not discussed in this work and the controller is designed to operate at a single frequency which does not allow the use of a droop control on the frequency.

Analysis of droop based generation control schemes for distributed generation inverters utilizing the conventional real power-frequency and reactive power-voltage droop control is presented in [20]. The paper develops small-signal models consisting of several distributed energy sources in a chain topology. It is a radial network of *n* generators with an infinite bus at one end and loads connected at each distributed resource bus. A system matrix for the microgrid is portioned into submatrices referring to the active and reactive power flows. An eigenvalue analysis and sufficient conditions were developed to

guarantee their small signal stability, and guidelines are provided for design of the active power-frequency and reactive power-voltage controllers. The paper shows that for the real power-frequency submatrix to be stable it is sufficient that the controller parameters be positive. The controller parameters for this loop are two variables related to the droop gain and the restoration loop time constant. The sufficient condition for stability in the reactive power-voltage submatrix is that the maximum droop in voltage of the k^{th} generator be less than its nominal value and the controller parameters are positive, the parameters being a constant term influencing the voltage droop and the controller filter corner frequency. The authors of the paper used IEEE 1547 performance specifications in the design process so that the microgrid would follow established regulations. No simulations or experiments were presented to verify the results of the mathematical proposition.

Using the analysis of line phasor dynamics can improve the stability of a grid with distributed generators beyond the conventional droop control [21]. Assuming the generators on the electrical system are three-phase voltage source inverters with PWM output filters, the generator is treated as an ideal voltage source with controllable frequency and voltage. If a low-pass filter is included on the output to reduce harmonics, the frequency control system resembles a classical model of a rotating generator with inertia and damping torque, both dependent on the droop gain. Root locus plots show that it is generally very difficult to obtain stable behavior for large droop gains since only the cutoff frequency of the low-pass filter can be adjusted. The authors present a compensator based on the line phasor model that introduces an additional three

parameters and that enables the controller design for voltage and frequency, while ensuring their stability. Simulations in the paper show the improvement in stability with improved performance in overshoot and settling time.

The microgrid model that this work focused on was a stand-alone microgrid with low-inertia rotating prime movers. A stand-alone system may be described as one in which the entire power is delivered to the system through energy sources operating with no connection to a larger reference grid. Typically the high-inertia generators in a large grid provide a reference frequency that is constant and a phase angle for a microgrid to determine if it should disconnect and reconnect. In a standalone system all the machines need to operate to provide a stable frequency and voltage in the presence or arbitrarily varying loads. The low inertia of the electrical system implies that large load steps will impose changes in the speed of the generators, creating fluctuations in system frequency. The previously listed works have dealt with an inverter between the energy source and the electrical distribution system. While simulations and experimental data have shown that droop control can be effective in controlling power distribution in a microgrid using inverters, there has been little work focused on rotating machines connected directly to the system and how their behavior is affected by droop control. Also, while some of the works have alluded to instability due to improper droop gains, this work will show through simulation and experiments that an improper selection of droop gain can cause problems in both system stability and individual machine performance.

2. DROOP CONTROL

For power systems based on rotating generators, frequency and active power are closely interconnected. A load increase implies that the load torque increases without a corresponding increase in the prime mover torque, which means that the rotational speed, and directly the frequency, decreases. The slowing of frequency with increased load is what a droop control is trying to achieve in a controlled and stable manner.

2.1 Background of Droop Control

To initially approach the origin of the droop control, consider the problem of complex power transferred by a transmission line. The transmission line is modeled in Figure 2 as an RL circuit with the voltages at the terminals of the line being held constant.

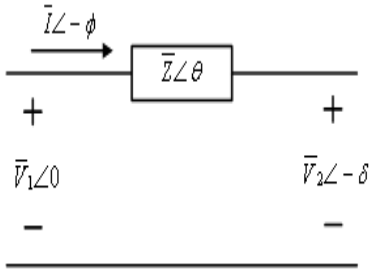

Figure 2. Power Flowing through a Line

The power flowing into a power line at the terminal is described by the equation

$$\bar{S} = P + jQ = \bar{V}\bar{I}^{*} = \bar{V}_1\left(\frac{\bar{V}_1 - \bar{V}_2}{\bar{Z}}\right)^{*}$$

$$= V_1\left(\frac{V_1 - V_2 e^{j\delta}}{Ze^{-j\theta}}\right)$$

$$= \frac{V_1}{Z}e^{j\theta} - \frac{V_1 V_2}{Z}e^{j(\theta+\delta)} \quad . \qquad (1)$$

Using Euler's formula to break the total power into real and imaginary components gives the real and reactive power flowing through the line to be

$$P = \frac{V_1^2}{Z}\cos\theta - \frac{V_1 V_2}{Z}\cos\ \theta + \delta \tag{2}$$

$$Q = \frac{V_1^2}{Z}\sin\theta - \frac{V_1 V_2}{Z}\sin\ \theta + \delta\ . \tag{3}$$

Further defining the line impedance to be $Ze^{j\theta} = R + jX$, the equations can be written as

$$P = \frac{V_1}{X^2 + R^2}\left[R\ V_1 - V_2\cos\delta\ + V_2 X\sin\delta \right] \tag{4}$$

$$Q = \frac{V_1}{X^2 + R^2}\left[X\ V_1 - V_2\cos\delta\ - RV_2\sin\delta \right]. \tag{5}$$

Typical transmission lines are modeled with the inductance being much greater than the resistance so the resistance is commonly neglected. The equations can then be written as the well known equations

$$P = \frac{V_1 V_2}{X}\sin\delta \tag{6}$$

$$Q = \frac{V_1^2}{X} - \frac{V_1 V_2}{X}\cos\delta\,. \tag{7}$$

If the power angle δ is small, then the small angle formula can be used so that sin δ = δ and cos δ = 1. Simplifying and rewriting the equations gives

$$\delta \cong \frac{XP}{V_1 V_2} \tag{8}$$

$$V_1 - V_2 \cong \frac{XQ}{V_1}\,. \tag{9}$$

Equations (8) – (9) show that the power angle depends heavily on the real power and the voltage difference depends on the reactive power. Stated differently, if the real power

can be controlled, then so can the power angle, and if the reactive power can be regulated, then the voltage V_1 will be controllable as well. In the droop method, each unit uses the frequency, instead of the power angle or phase angle, to control the active power flows since the units do not know the initial phase values of the other units in the stand-alone system. By regulating the real and reactive power flows through a power system, the voltage and frequency can be determined. This observation leads to the common droop control equations

$$f = f_0 - k_p \left(P - P_0 \right) \tag{10}$$

$$V_1 = V_0 - k_v \left(Q - Q_0 \right) \tag{11}$$

where f_0 and V_0 are the base frequency and voltage respectively, and P_0 and Q_0 are the temporary set points for the real and reactive power of the machine. The typical droop control characteristic plots are shown in Figure 3.

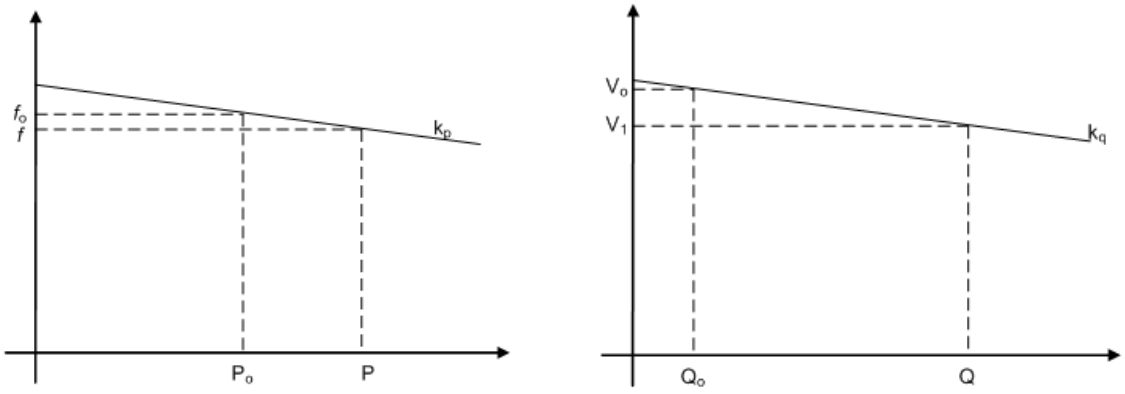

Figure 3. Droop Control Characteristic Plots

From the droop equations and highlighted by Figure 3, as the real power load on the system increases, the droop control scheme will allow the system frequency to decrease. In the droop control, it should be noted that the droop method has the inherent trade-off between the active power sharing and the frequency accuracy, resulting in the frequency

deviating from the nominal frequency. It would be desirable to create a controller that would restore the frequency to the nominal frequency after a disturbance and such a controller for inverters was proposed by Chandorkar et al. [22]. Frequency restoration is not practical in systems with inverters due to the inaccuracies in inverter output frequency [23]. These minor differences in inverter's frequency result in increasing circulating currents creating an unstable system. However, a system with rotating machines may lend itself to a droop control with frequency restoration.

If an active power controller is built to include a frequency restoration loop, the controller is analogous to an engine governor. Engines are equipped with governors to limit the engine to a maximum safe speed when unloaded and to maintain a relatively constant speed despite changes in loading. As the load varies, the speed may droop but over a period of time will return to its nominal speed.

2.2 Droop Control Modifications

One assumption made in the original calculation of the common droop control equations is that the inductance in the line is much greater than the resistance. This is a good approximation with high-voltage transmission lines, but a microgrid can operate at a lower voltage with cables that have resistances that cannot be neglected. Table 1 lists typical line parameters R, X and the typical rated current for the high, medium, and low voltage lines [24]. A medium voltage line has mixed parameters and the low voltage lines are predominantly resistive. To create of more general droop control both the resistance and reactance should be considered.

Table 1. Typical Line Parameters

Type of Line	R (Ω/km)	X (Ω/km)	I_N (A)
Low Voltage Line	0.642	0.083	142
Medium Voltage Line	0.161	0.190	396
High Voltage Line	0.06	0.191	580

Brabandere et al. [25] propose a transformation that is an orthogonal linear rotational transformation matrix **T** to create a new active and reactive power, *P'* and *Q'*

$$\begin{bmatrix} P' \\ Q' \end{bmatrix} = \boldsymbol{T} \begin{bmatrix} P \\ Q \end{bmatrix} = \begin{bmatrix} \sin\theta & -\cos\theta \\ \cos\theta & \sin\theta \end{bmatrix} \begin{bmatrix} P \\ Q \end{bmatrix}$$

$$= \begin{bmatrix} X/Z & -R/Z \\ R/Z & X/Z \end{bmatrix} \begin{bmatrix} P \\ Q \end{bmatrix}. \tag{12}$$

This transform results in the equations

$$\sin\delta \cong \frac{ZP'}{V_1 V_2} \tag{13}$$

$$V_1 - V_2 \cos\delta \cong \frac{ZQ'}{V_1}. \tag{14}$$

From Equation (13), it can be seen that by regulating *P'*, the power angle δ and thus the frequency is controlled, whereas regulating *Q'* controls the voltage V_1. Figure 4 shows the relationship between *P'*, *Q'*, *P* and *Q*.

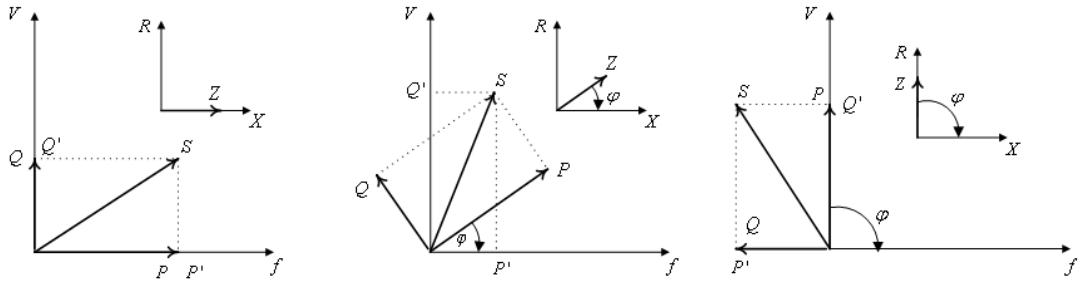

Figure 4. Torque and Power Curve for Diesel Engine

From Figure 4 it can be seen that if $X >> R$, then the relationship stays the same and $P' = P$. However as the resistance in the lines increases and becomes the dominant term, $P' \cong -Q$ and $Q' \cong P$. The new droop control equations become

$$f = f_0 - k_p \frac{X}{Z} \left(P - P_0 \right) + k_p \frac{R}{Z} \left(Q - Q_0 \right) \tag{15}$$

$$V_1 = V_0 - k_q \frac{R}{Z} \left(P - P_0 \right) - k_q \frac{X}{Z} \left(Q - Q_0 \right) . \tag{16}$$

The new equations show that the frequency will be dependent on the real and reactive powers as well as the ratio of the impedances in the line. It is sufficient that the ratio of the ratio of impedances is known, so the actual values are not necessary for the droop control.

This modified droop control can be extended to inverters tying renewable energy sources to the grid. In a low-voltage system the transmission lines appear to be resistive output impedance on an inverter. While the droop method has been studied in parallel dc converters, little work has been done in the application of the resistive droop method to parallel inverters [26]. The advantages of using the new droop control are the following: (1) The overall system is more damped. (2) It provides automatic harmonic current sharing when using inverters. (3) Phase errors barely affect active power sharing.

3. MODELING AND SIMULATION

3.1 Issues with Commercial Power Flow Solutions

Power system analysis is typically done using commercial software that performs power distribution, transient stability and fault analysis by obtaining a power flow solution. However, commercial power flow models will not work well in the study of stand-alone microgrids. Power flow models make two assumptions that are not acceptable for the modeling of microgrids operating under a droop control:

- The existence of the slack bus
- A constant frequency

Typically, power flow models have three types of buses: a slack bus, a generating bus and a load bus. At a generating bus the active power and voltage magnitude may be specified by varying the mechanical torque and generator field current. All other buses specify real and reactive power. Generally all the real power values at all the buses cannot be specified independently due to the requirement for power balance. The power at the slack bus is left open "to take up the slack" and balance the change in real power and provide a reference to the rest of the generators in the system [27]. The slack bus is not viable in a stand-alone system since any change in power requirements needs to be evenly distributed among the generators.

The changing frequency will influence the power flow solution. The difference in frequency will influence the machine dynamics through Equation (17).

$$\frac{d\delta}{dt} = \omega - \omega_s \tag{17}$$

where:

ω electrical frequency of the machine [rad/sec]

ω_s temporary set-point for synchronous speed of the system [rad/sec]

The angle of the rotating shaft δ is included in both the network equations and stator algebraic equations that are used to solve for the voltage and power angle at a particular bus. This leads to the conclusion that a varying frequency will influence the voltage magnitude and angle. The degree of influence is beyond the scope of this work but more information can be found in [28]. It is sufficient to realize that traditional power flow solutions are too incomplete to study the steady-state behavior of a stand-alone microgrid.

3.2 Electric Machine Model

The electric machine used in the generator model for this study was a basic model of a current-dependant voltage source behind impedance [29].

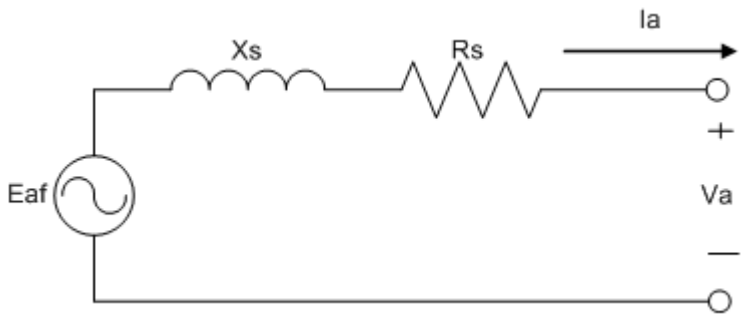

Figure 5. Simplified Model of a Synchronous Machine

For this model in Figure 5, it is assumed that the stator resistance is negligible and so the stator only has an inductive reactance. The terminal voltage, V_a, is held constant by a

voltage regulator while the internal voltage is varied by the field current and speed of the machine through the equation

$$E_{af} = \frac{\omega_e I_f L_{af}}{\sqrt{2}} e^{j\theta} \tag{18}$$

where:

ω_e Angular frequency of the applied electrical excitation [rad/sec]

I_f Dc excitation in the field winding

L_{af} Mutual inductance between the field winding *f* and phase *a*

θ Electrical angle of the rotor

The speed of the generator is determined by the prime mover. The relationship between the speed of the prime mover ω_m and the electrical speed ω_e is given by

$$\omega_m = \frac{2}{poles} \omega_e . \tag{19}$$

Generator sets currently use a four pole machine to generate power so the angular speed of the system will be twice the speed of the shaft of the prime mover. The nominal frequency of the microgrid will be 60 Hz – or 377 rad/s, 3600 rpm – so the prime mover should have a speed of 1800 rpm.

3.3 Model of the Droop Control on a Prime Mover

To observe the behavior of a generator set on a droop control scheme, a model was created that modeled a prime mover driving a rotating generator connected to an ac grid with varying frequency, as shown in Figure 6.

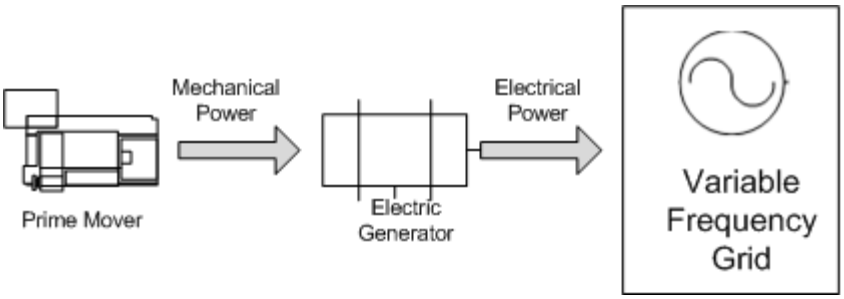

Figure 6. Model of Genset Connected to an Ac Grid

The droop control is referenced to the prime mover, not the electrical generator, and rewriting the original droop equation reveals that the power out of the prime mover can be stated by the equation

$$P = P_0 + \frac{\omega_0 - \omega}{k_p}. \tag{20}$$

P_0 and ω_0 are pre-determined set-points that are known, so it follows that if the speed of the system is known, output power of the generator can be determined. The set-points of the droop control are chosen for a particular application and can be changed by an operator or the controller if disturbances are present or if the configuration of the system changes, such as adding loads or generators.

While equation (20) can be used to find the power out of the prime mover, the speed of the system needs to be determined. How the speed of the system changes with load disturbances can be found using the dynamic relationship shown in Equation (21).

$$\frac{d\omega}{dt} = J \int P_{load} - P_{generated} \; dt. \tag{21}$$

If the load requires more power than is being generated at that time, the speed of the machines on the system needs to increase to meet the demand. For modeling and

simulation, P_{load} and $P_{generated}$ were calculated for the entire system; the dynamic speed is for the system, not for the individual machines.

The inputs to the unit are the speed set point, power set point, system load requirements P_{load}, and the power generation from the other units. The load also includes any losses in the system. The power generated by other units is given by

$$P_g = \sum_{\substack{k=1 \\ k \neq i}}^{n} P_k \tag{22}$$

where:

n number of generators operating on the system

P_g Total power generated on the system minus the generator being simulated

P_k Power generated out of the k^{th} generator on the system

The block diagram for the model of a prime mover with droop control is shown in Figure 7.

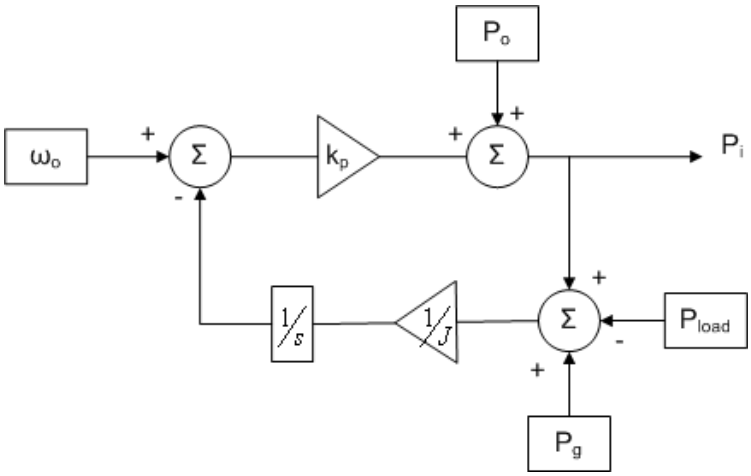

Figure 7. Block Diagram for Prime Mover with Droop Control

3.4 Transfer Function Analysis of a Machine on Droop Control

The system in Figure 7 can be represented by the transfer function shown in Equation (23).

$$P_i = \frac{1}{k_p}\left(\frac{s}{s+\frac{1}{Jk_p}}\right)\omega_o + \left(\frac{s}{s+\frac{1}{Jk_p}}\right)P_o + \frac{1}{Jk_p}\left(\frac{1}{s-\frac{1}{Jk_p}}\right)P_g - P_{load} \quad . \qquad (23)$$

From the transfer function it is seen that there are two zeros at the origin, two poles at $s = -\frac{1}{Jk_p}$ and one pole at $s = \frac{1}{Jk_p}$. The pole in the right half-plane can cause instability in the system and so it would be desirable to move that pole into the left half-plane. Since the inertia is set by the machines on the system, the droop gain k_p is the only method of creating a more stable system. Inserting a transfer function in place of the droop gain would be one way to move the unstable pole to the right half-plane. A simple alternative is to change the droop gain from a simple proportional gain to one that resembled a high pass filter shown in Equation (24).

$$G(s) = \frac{sk_p}{sk_p + 1}. \qquad (24)$$

The new transfer function is now represented by

$$P_i = \left(\frac{sJk_p}{sJk_p + J + k_p}\right)\omega_o + \left(\frac{J\ sk_p + 1}{sJk_p + J + k_p}\right)P_o + \left(\frac{k_p}{sJk_p + J + k_p}\right)P_{load} - P_g \quad . \qquad (25)$$

All the poles in the new transfer function are in the left hand-plane, creating a more stable system and there is now one zero at the origin and another zero at $s = -\frac{1}{k_p}$. It should be noted that while the droop gain k_p is a factor in establishing stability, the inertia of the

entire system is another important component in creating a stable system. Computer simulations in the following section will briefly explore some of these concepts.

3.5 Computer Simulations of Droop Control in a Microgrid

To initially see how different droop gains and low inertia values affect microgrid systems, a computer simulation was created in Matlab and ran using different droop gains and controller configurations. The prime movers used in the simulation had a power output determined by the droop equation introduced in Section 3.3 and the nominal power set point was set at 61.7 kW. The four pole generator has a series reactance of 1.68 Ω, a mutual inductance of 0.0223 H, and an initial power factor of 0.85. The terminal line-to-line voltage was 460 V. Figure 8 shows the frequency behavior through a load step on the system. The frequency finds its initial steady state value at approximately 59.5 Hz and again reaches a steady state value at 54.4 Hz after the load step. Figure 9 shows that the power output is equally distributed among the generators when they have the same droop gain.

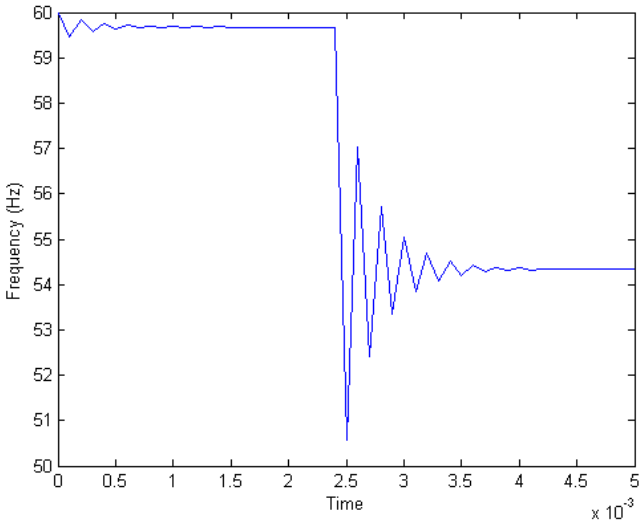

Figure 8. System Frequency under a Changing Load

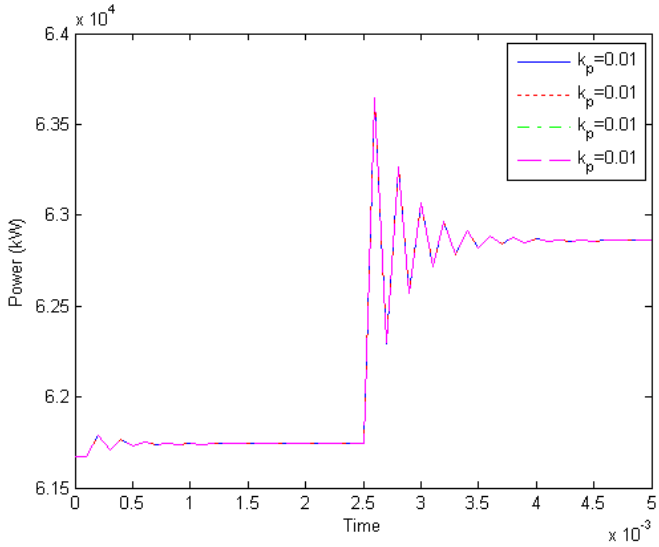

Figure 9. Generator Power under a Changing Load with Similar Droop Gains

Combined, the figures show that as the power output of the generators increased to meet an increase in load demand, the system frequency decreased as required by the droop gain. Power distribution becomes unbalanced in the system when the droop gains on the different generators are varied, as illustrated in Figure 10.

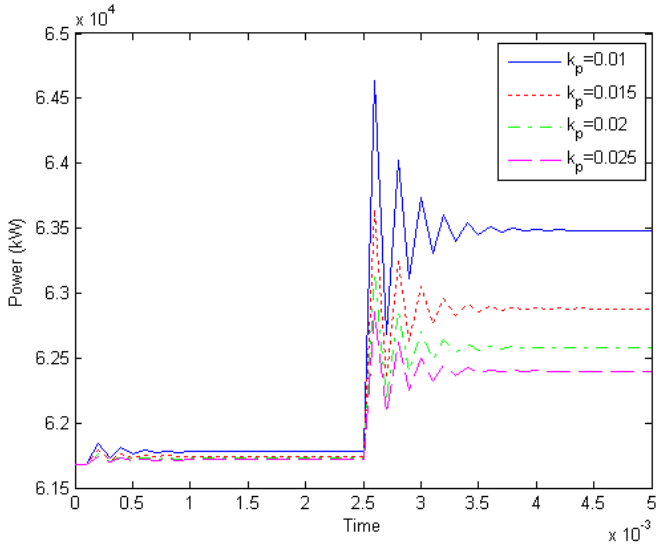

Figure 10. Generator Power under a Changing Load with Different Droop Gains

The imbalance in power distribution is expected from the droop equations. The power out of the generator is determined by the droop gain since the operating frequency and set points are the same for all generators. It follows from Equation (20) that the generator set with the lowest droop gain will inject the most power into the system, and this is confirmed in Figure 10. The simulation also shows that the further the generators move from their set points – 61.7 kW in this case – the larger the power difference between generators.

The previous simulations have shown that the power and frequency reach a steady state that is stable operating point; however, previous analysis of the system transfer function suggests that the droop gain can influence the stability of the system. To explore that concept further, the droop gain for all machines is decreased to $k_p = 0.01$ while keeping all other parameters the same and the system becomes unstable as shown in Figure 11.

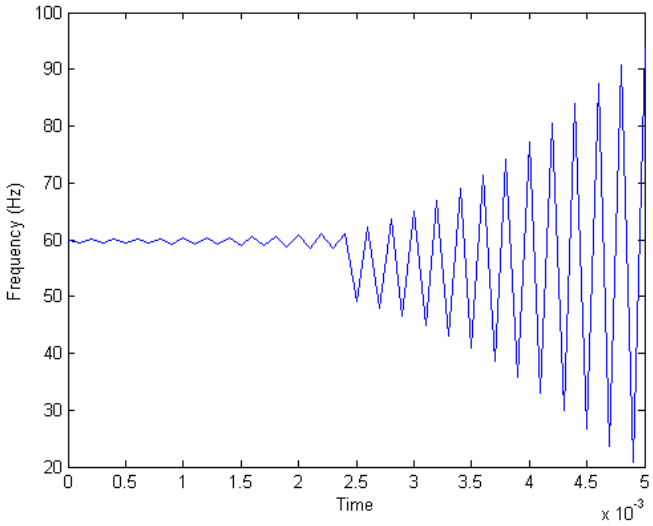

Figure 11. Frequency with All Machines at Droop Gain $k_p = 0.01$

The instability can be resolved by using a droop control function similar to a high pass filter instead of a simple proportional gain as discussed in Section 3.4. The new block diagram for the system is shown in Figure 12 and the frequency behavior of the system with the improved droop controller is given in Figure 13.

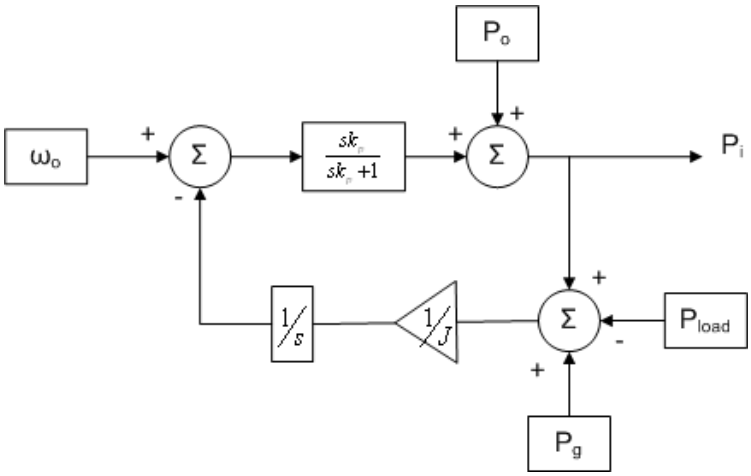

Figure 12. Block Diagram with Improved Droop Controller

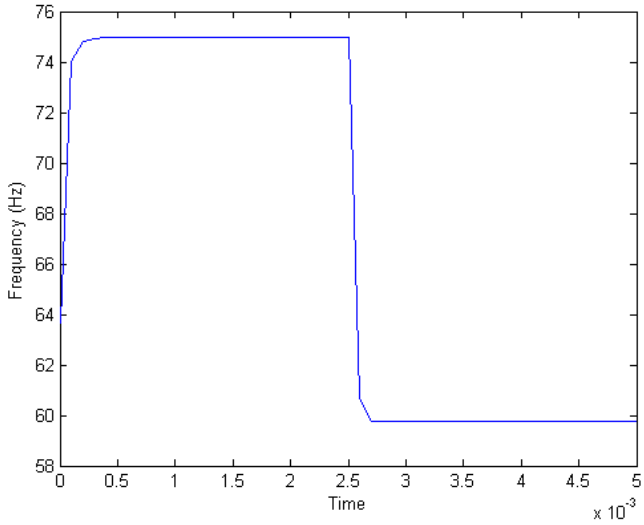

Figure 13. Frequency with a Filtering Droop Control

The frequency of the new system is slower to change but remains stable through the same load steps as before with a k_p = 0.01, lending credence to the idea that a droop control in the form of a filter can further improve system stability.

4. EXPERIMENTAL RESULTS

4.1 CERTS Microgrid

The use of droop control to create a stable electrical system is not a new concept and one large-scale test has been the field verification of the Consortium of Electric Reliability Technology Solutions (CERTS). The CERTS microgrid program used developed control methods to allow the installation of distributed generators in a plug-and-play manner [30]. The microgrid consists of a static disconnect switch that isolates the distributed sources from the utility grid. The islandable part contains two loads and two inverter-based sources on one feeder and a single load and source on the parallel feeder. A one-line diagram of the system is shown in Figure 14.

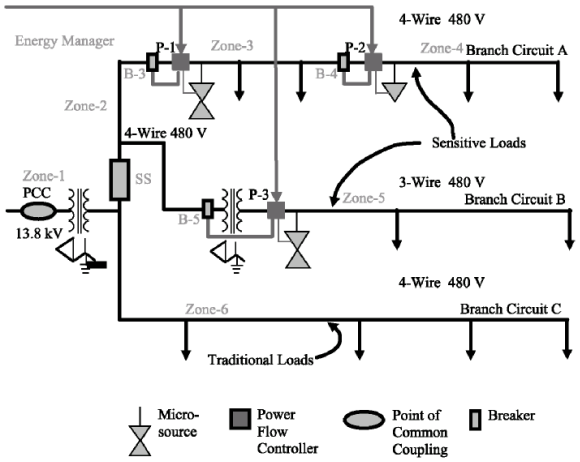

Figure 14. CERTS Microgrid Test Bed [31]

The generators on the microgrid are capable of producing 60 kW and are being driven by 7.4 liter, naturally aspirated V-8 engines, specially designed for natural gas. The power from the rotating machine generators is run through a diode rectifier and boost, then inverted to achieve the desired ac signal. The four loads on the system – one load designated as non-critical – can be controlled from 0-90 kW and 0-45 kVar. Other loads

on the system include an induction motor 0-20 HP, a harmonic injection using a three phase diode bridge and a digital dc load. Other equipment includes transformers for operating at the correct voltage level, protection relays, shunt trip breakers and a data acquisition system.

The CERTS microgrid, hosted by American Electric Power, was subjected to five sets of tests by the developers: (1) to examine the operation of the static switch to determine that it and its digital signal processing control operated as designed; (2) to examine a preliminary set of faults within the microgrid to ensure protection and safety of the test bed prior to performing other tests; (3) to ensure that the Gen-set inverter controls are working as designed during grid-connected and islanded modes of operation; (4) to demonstrate the flexibility of the microgrid both while connected to the grid and islanded, for different loads, power flows, and utility impact; (5) to explore the operational limits of the microgrid with difficult induction motor starting loads [32]. The series of tests performed confirmed the CERTS microgrid concepts of achieving seamless transitions from grid-tied to islanded modes of operation, an approach to electrical protection within the microgrid and a method for microgrid control that does not depend on high-speed communication. The concept of using a droop control within the context of microgrids is further explored experimentally in the following sections.

4.2 Experimental Set-up

The CERTS microgrid is a good test bed and validation of some key microgrid concepts. This work focused on a stand-alone system that would not have the utility grid as a reference and with little pre-engineering could become a mobile electrical supply system.

The experiment was tightly constrained with only one type of prime mover and generator, confirmed the behavior of the droop control and explored how different droop gains could impact power distribution. A diagram of the experimental system is shown in Figure 15.

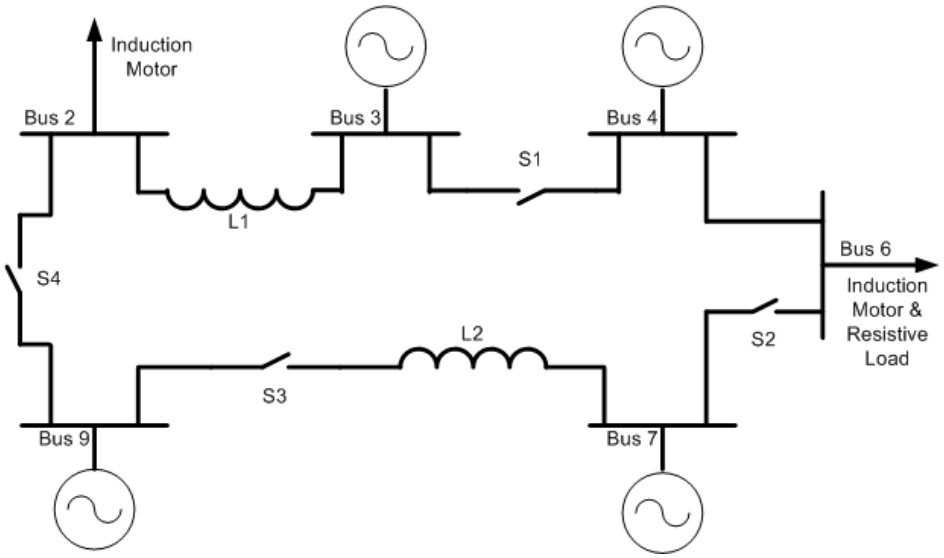

Figure 15. Radial Microgrid Structure for Experimentation

There are four low-inertia 1 kW generators connected in a radial system, each being driven by a permanent magnet dc servomotor. A LabVIEW interface allows the operator to set either the velocity or torque for the dc servomotor. The interface allows the operator to monitor the speed, power, current and torque of the dc servomotor. While operating in speed mode, an option was available to turn on the droop control with the entered droop gain. This was done to quickly study the effect of a change in the droop gain slope as well as reverting back to the traditional configuration of using a generator in speed mode as a slack bus.

The dc servomotor is connected to the shaft of the generator by a rubber coupling. To simulate line inductance, two three-phase inductors were inserted into the system, each inductor having a value of 1.86 mH per phase. Fast-acting fuses were employed to protect the equipment from excessively high current. There were three-phase switches employed between generator sets for synchronization purposes. Upon system start-up, a generator was brought up to speed by setting the desired speed in the LabVIEW interface and maintaining proper voltage control by adjusting the field current. Once the initial generator was online, the switches on either side of the generator were closed to connect the generator to the adjacent buses. During this time, the remaining generators were not connected to their respective buses. Once power was at a bus, the dc servomotor's torque was increased until it reached the proper speed, voltage and phase and then it was connected to the bus, synchronizing it to the system.

Once the four generators on the system were synchronized, the system loads were applied. There were two types of loads on the system, two induction motors and a resistor box. The induction motors provided a load determined through the same LabVIEW interface that controlled the generator. In this case, instead of acting as the prime mover, the dc servomotor provided a constant torque on the induction motor creating a base load for the system. The resistor boxes consisted of 10 resistors in parallel providing resistances from 500 Ω to 50 Ω. Electrical power measured out of the generators was calculated using the two-wattmeter method. The droop controller was implemented within the LabVIEW program and used the power out of the dc servomotor

as a feedback signal to be multiplied by the droop gain in order to calculate the change in frequency.

The goals of the demonstrations were to:

- Validate that the droop control functioned as expected
- Investigate how different gains in the droop controller effected the system's power distribution
- Establish if a droop controller could increase the stability of a low-inertia microgrid

4.3 Effect of Droop

The initial experimental run consisted of one of the generators acting as the slack bus and the other three generators operating in torque mode. On the slack bus a speed of 1200 rpm was entered into the velocity command box in the LabVIEW controller, setting the frequency of the system at 60 Hz. The other generators in the system were operating in torque mode and operators manually adjusted the torque to maintain power balance between the four generators. The two induction machines provided a load to the system by each maintaining a constant torque of 2.5 Nm on the system. The resistor boxes then provided load steps of known value, as previously stated. Figure 16 shows that the system maintains a speed of 1198 rpm through different loads on the individual generators ranging from 20 – 742 W.

To test that the droop control functioned properly, the control was activated on the generator at the slack bus. Procedures for testing remained the same as the previous experiment. The power versus speed data from the droop control is shown in Figure 17.

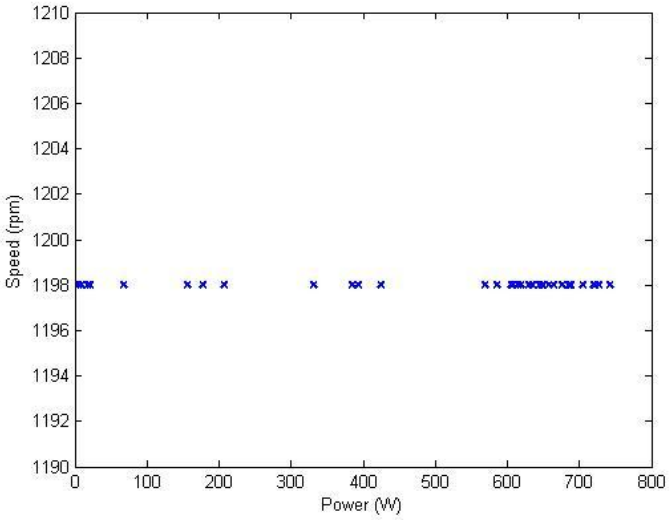

Figure 16. System with No Droop Control

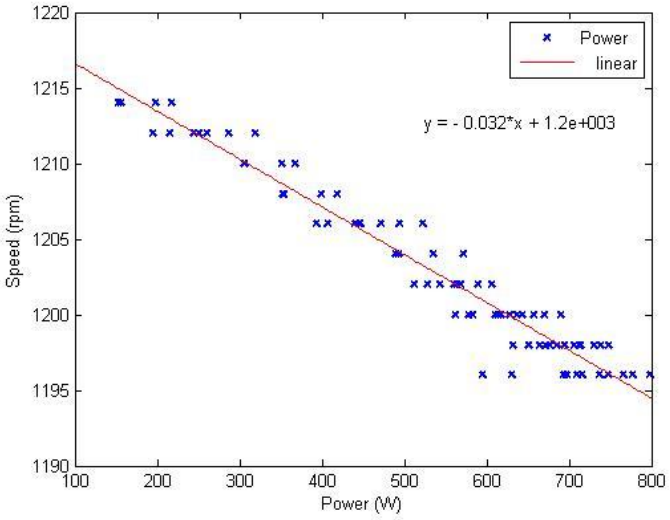

Figure 17. System with All Generators on Droop Control with Droop Gain k_p = 0.03

Additional verification of the droop control came with an experimental setup that consisted of one generator on droop control with the remaining generators on torque

mode. The load was then increased or decreased in a random manner to be sure that the system would respond correctly. The speed of the generator at the slack bus is shown in Figure 18. The sampling rate is set internally by LabVIEW and the data is from the speed and power of the dynamometer.

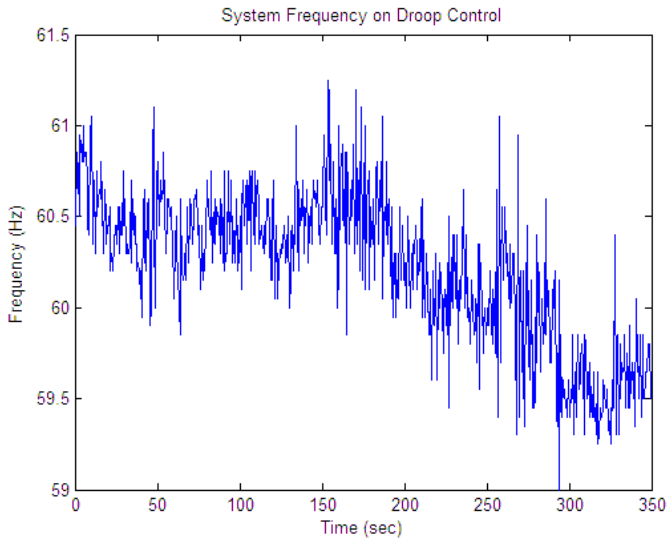

Figure 18. System Frequency Response over Random Load Changes

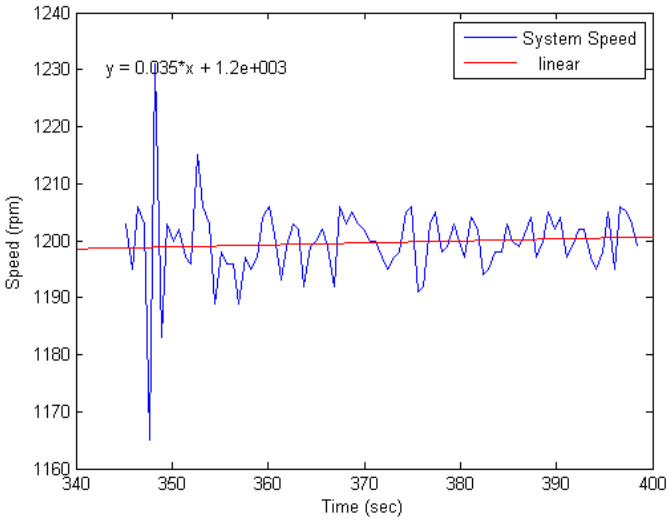

Figure 19. System Speed after an Increase in Load

Figure 19 illustrates the behavior of the speed of a generator on droop control after an increase in load. The speed fluctuates immediately following the load change from 1165

rpm to 1230 rpm and then settles down and increases at a slope of 0.035 which is close to the droop gain of $k_p = 0.03$.

4.4 Increased Stability with Droop Control

System stability with a droop control was examined using the load steps provided by the resistor boxes. The ability to handle a load step without collapse will be used to determine the stability of a system for this exercise. Voltage collapse should not be a part of the system since the voltage was actively regulated by varying the field current manually in each generator to maintain proper line voltage. System collapse happened when the generators lost synchronism and a generator's speed went to zero or attempted to go to infinity.

The base load for the system was the induction motors providing torques of 2.25 and 2.5 Nm giving a base electrical load of 2420 W. The generators were to maintain a speed of 1200 rpm through any load dynamics. With no resistive load introduced into the system, the four generators provided 2375 W as measured at the generators and 3026 W at the dynamometer. Resistive load was added to the system, and once it was determined that the system could handle the load step, the system was brought back to the base load and then a larger load step was imposed on the system. The system with no droop control was able to maintain its synchronism with a change in load of five resistive steps totaling a maximum load step of 122 W. The system lost synchronization with the next load step which would have been approximately 153 W.

The droop control was introduced into the system one generator at a time. The first run was done with the generator at the slack bus on droop and the remaining three in torque mode. A second run was done with two generators operating in speed mode with the droop control activated and the remaining generators providing power balance through torque variation, and so on, until all four generators operated under droop control. The droop gain, k_p, was kept constant for these experiments. With the droop control enabled on the generators the system could sustain a load step of 152 W without collapse, a 25% increase in load step over the system operating with droop control. Using this criterion the droop gain was able to provide a more robust microgrid.

The number of generators operating with a droop controller did not noticeably increase the amount of load step the system is capable of handling. For two, three or four generators operating on droop control, the system lost synchronism with a load step around 152 W. The difference in behavior came with how the microgrid collapsed. If there were multiple generators on droop control, the generators operating with a controller did not lose synchronism. During a system collapse the generators operating in the torque mode would lose synchronism and then speed up attempting to maintain the constant torque that was the input. Since the generators on droop control were still synchronized after system collapse, they provided a reference point to brown start the microgrid since there were already synchronized generators on the system. In this way, a droop control may be a way to decrease the chances of a total blackout.

A system with all four generators on droop control behaved slightly differently since no generators were operating in torque mode, and so no generators lost synchronism immediately after an overload of the system. The stability of the system with all four generators on droop control was contingent on ensuring that the voltage was regulated. During the multiple experimental runs, the main cause of collapse with all generators on droop control was improper voltage control. The voltage was being maintained by the operators at each generator by increasing the field current in the generators. If the operators neglected to monitor the system voltage, a voltage collapse would occur. However, the droop control did assist in an important area here as well. Figure 20 shows that the speed originally decreases after a load change but at a slow enough rate that the operator was given time to change the field current on the generators to maintain rated voltage, preventing a system collapse.

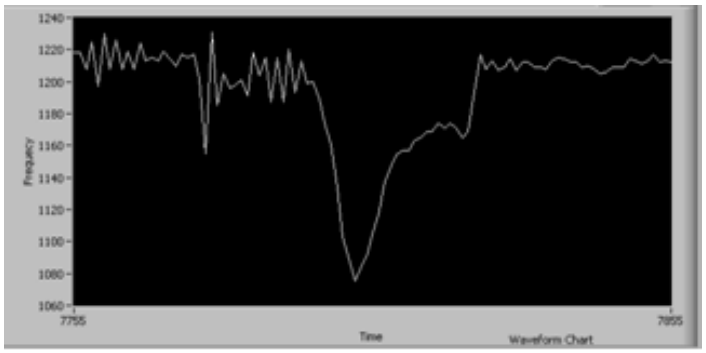

Figure 20. Speed Recovery with No Lightening of the System Load

4.5 Effect of Different Droop Gains on the System

4.5.1 Effect of Increasing or Decreasing System Droop

The value of the droop gain for the system is determined by a desired speed slope. From the droop control in Equation (10) it is easy to solve for the droop gain given a desired speed at a desired power output. For example, if the expected speed at 500 W is to be

1200 rpm, then P_0 is 500. If the desired speed at 1000 W is 1180, then those values can be inserted into the droop equation and the droop gain is determined to be k_p = 0.04. In a trivial case, with a droop gain of zero the system acts as though no droop control was imposed on the system. It follows that if the droop gain is not sufficiently large, the system does not increase its ability to handle large step loads. At the same time, if the droop gain is too large, small changes in the load would cause large fluctuations in the system frequency with the possibility of a system collapse. It is critical to find the range of the droop gain that can give enough stability to handle load steps while at the same time not imposing radical changes in the system frequency.

Different droop gains also impacted the microgrid by creating an oscillating frequency. For a second round of experiments the base load was changed so that the torque on the two induction motors providing the base load was 1.5 Nm for each machine. The generators operated with a droop gain of k_p = 0.03, the same gain as in previous experiments. With the lighter loading of the system, the system speed oscillated as shown in Figure 21.

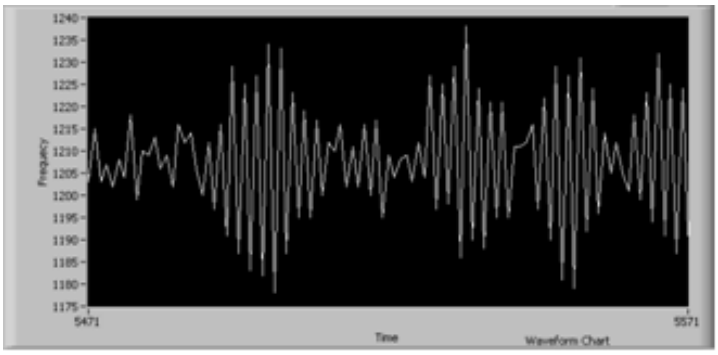

Figure 21. Speed of Lightly Loaded System with Droop of 0.03

When the droop gain was decreased to $k_p = 0.02$, the oscillation in the speed would decrease to a steady state. Figure 22 shows the transition of the system when the droop gain is decreased from 0.03 to 0.02.

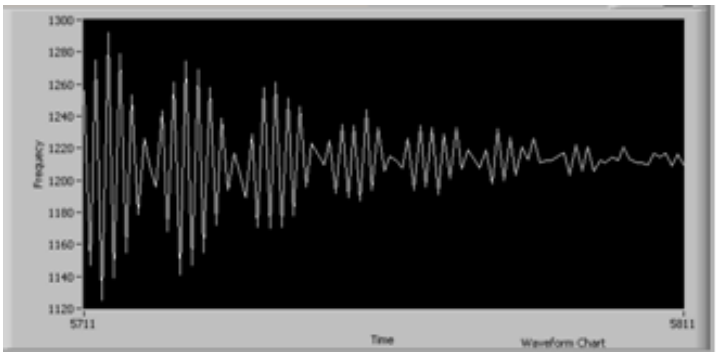

Figure 22. System Speed as Droop Gain Decreases from 0.03 to 0.02

The system was stable in previous tests that involved a system with a greater base load and operated with a droop gain of $k_p = 0.03$. Once the base load was decreased, the system reached an unstable operating point causing the frequency to oscillate. Decreasing the droop gain to $k_p = 0.02$ while the system is at the previous unstable operating point brings the system to a stable operating point where the frequency goes to a steady-state value. The results are not totally unexpected. In Section 3.4, it is shown that there exists an unstable pole that is dependent on the inertia and droop gain related to the system loading. The decrease in system loading moved the pole into an unstable region and the decrease in droop gain moved the unstable pole back into a stable region.

4.5.2 Different Droop Gains within the Same System

The droop control states that the power and frequency out of the generator set is determined from the frequency droop. A synchronized system implies that the frequency is the same for all machines and that the power will be evenly distributed between the generators and prime movers on the system. The only variance in the system comes from

the droop gain k_p, and it follows that if a gain is imposed on a generator within the system that is different than the other machines, then the power output will be different as well.

Using the same microgrid as previous experiments, two generators were put on droop control and the other two generators were operated in the torque mode. One induction motor provided a base load that was increased to observe how the torque of the different generators was affected. The operators attempted to keep the torque of the two generators operating in torque mode between the torques of the two generators in droop control. Table 2 shows how the torque was distributed across the generators when both operated with the same droop gain.

Table 2. Torque Balance between Machines with Equal Droop Gain

Load Torque	Machine 3 Torque Mode	Machine 4 $k_p = 0.04$	Machine 7 Torque Mode	Machine 9 $k_p = 0.04$
0	1.525	1.74	1.48	1.635
0.5	2.025	2.47	1.975	2.36
1.05	2.515	2.75	2.47	2.595
1.55	3.015	3.05	2.97	2.92
2.05	3.265	3.64	3.22	3.505
2.55	3.77	3.97	3.705	3.885

Table 3 shows the same system as before but with the droop gain of one of the generators set at $k_p = 0.04$ and the other generator operating with a droop gain of $k_p = 0.01$. Comparing Table 2 and Table 3 it is obvious that operating with a different droop gain on different machines within the same system creates an imbalance in torque, and thus

power output, between the different generators. This can be expected if the system is synchronized since the droop equation relates the power out of a generator to the droop gain at a determined speed. The difference in torques between Machines 4 and 9 in Table 3 is greater than expected from the simulations shown in Figure 10. The torque on Machine 9 is three times greater than the torque on Machine 4, while simulations show only a three percent difference between similar differences in droop gains. The difference between the desired speed of the controller and the synchronous speed of the generator is causing the greater than expected difference in torques, resulting in a significant loss of efficiency.

Table 3. Torque Balance between Machines with Different Droop Gains

Load Torque	Machine 3 Torque Mode	Machine 4 $k_p = 0.04$	Machine 7 Torque Mode	Machine 9 $k_p = 0.01$
0	1.52	0.81	1.48	2.75
0.5	1.765	0.99	1.73	3.5
1.05	2.025	1.24	1.98	4.4
1.55	2.27	1.46	2.23	5.56
2.05	3.53	1.435	3.47	5.23
2.55	4.025	1.24	3.96	4.34

An alternative test to study the effect of different droop gains within the same system is to set a base load and then change only the droop gain on one machine. Table 4 shows the data when each of the induction motors has a load of 1.5 Nm and the system is configured as before with two generators in torque mode and two generators operating with droop control. The droop gain is originally set to $k_p = 0.03$ for both machines and

the system is brought to a steady state where the load is shared equally among the generators.

Table 4. Torque Imbalance with Changing Droop Gain with Constant Load

Load Torque 1	Load Torque 2	Machine 3 Torque Mode	Machine 4 $k_p = 0.03$	Machine 7 Droop	Machine 9 Torque Mode
1.5	1.55	4.51	2.30	6.535 $k_p = 0.01$	4.50
1.5	1.55	4.51	3.60	5.225 $k_p = 0.02$	4.505
1.5	1.55	4.51	4.475	4.33 $k_p = 0.03$	4.50
1.5	1.55	4.51	5.13	3.705 $k_p = 0.04$	4.505

The data in Table 4 shows that the generator with the lower droop gain has the highest torque imposed upon it. This difference in torque can create issues with ratings, as seen on Machine 7 when the droop gain is set to $k_p = 0.01$. The torque limit of the generators is 7 Nm, and when the droop gains are equal it does not approach this limit; however when the droop gain is decreased, the torque approaches its limit creating a situation where the system load cannot be increased beyond the modest load already on the system without violating the ratings on a generator.

5. CONCLUSIONS

The use of distributed generation sources in a microgrid structure is one solution to the problem of providing reliable power where a main electrical grid is not present. Maintaining a stiff frequency with low-inertia generators in these microgrids can cause instability if the load step is too large. A droop control relates the change in system frequency to the active power produced by the generators by using only locally available information. A proportional gain controller improves the stability of the system by dampening the effect of rapid load changes, providing critical time for the system to adjust to prevent loss of synchronism.

There are problems with a simple proportional gain droop control due to the inherent right half-plane poles in the system's transfer function. These unstable poles can cause frequency oscillations or system collapse if the wrong value of droop gain is chosen relative to system loading, or if the inertia of the system is too low. Replacing the proportional droop gain with a function similar to a high-pass filter improves system response and stability by moving the unstable poles into the left half-plane. Experimental results showed that a system with a droop controller was more stable than a system maintaining a set frequency. Data also confirmed that a system comprised of generators operating with different droop gains had an imbalance in load sharing. This created problems with providing the required power without violating torque ratings on machines. Despite the potential of power imbalance, a system operating on droop control with the same droop gains provides an efficient, reliable method for delivering power to critical loads while maintaining stability through large load changes.

Within the context of this work, additional work could be done to create a better voltage management system. This could be approached in several ways, either maintaining a strict voltage level through constant management of field current or using the reactive power on the system to maintain the desired voltage similar to the second droop equation. Utilizing the microgrid configuration used in this work, it would not be difficult to explore what impact the modified droop equations have on a stand-alone system. While previous work has mentioned that frequency restoration with a droop control is unfeasible with inverters, no work has shown the effect rotating machines would have on a system with frequency restoration. Inserting an additional loop in the LabVIEW program to restore the frequency to the nominal speed would provide insight into the possibility of a stable system created from rotating machines with frequency restoration. The synchronism of rotating machines would decrease the amount of circulating currents, and any inverters on the system need only match the system frequency, eliminating the obstacles to frequency restoration in droop control.

There is a lot of future work that can be done to improve the analysis of microgrids. A complete power flow simulation needs to be developed similar to power flow programs commercially available for utility systems. This microgrid simulation should take into account the lack of a slack bus, changing frequency, and low-inertia generators, and it should be adaptable to implement a high penetration of renewable energy sources. Previous models of microgrids have focused on inverter sources, but it may not always be feasible or efficient to but a diode rectifier and inverter between a rotating generator and the electrical system. This may require including the full dynamics of rotating machines,

which is complicated but necessary because most of the mobile, dispatchable generator sets used to create a microgrid will be driven by diesel engines or natural gas turbines. A complete power flow solution could also investigate the impact of line impedance on the effectiveness of the droop equation, as alternative droop equations suggested in Section 2.2.

A universal control connection box is a goal for development research. A device that can take the input of any generator and connect that source to an ad hoc system, providing control to the generator using only local information, would allow a microgrid to be constructed using any available energy source. Be it a portable solar installation, diesel generator, microturbine or fuel cell, the power output would be connected to the input of a universal connection device and the connection device would regulate power output and voltage to maintain stability while maximizing the efficiency of the generators. Depending on the design of the connection device, a universal connection device would also be easier to model in a microgrid simulation because only the connection device would need to be modeled, not the energy source. Much work can be done to further understand the dynamics of microgrids, and completing the work will realize the full potential of combining distributed generation with microgrid concepts.

REFERENCES

[1] T. Ackermann, G. Andersson, and L. Soder, "Electricity market regulations and their impact on distributed generation," in *Proceeding on International Conference on Electric Utility Deregulation and Restructuring and Power Technologies*, 2000, pp. 608-613.

[2] T. Ackermann, G. Andersson, and L. Soder, "Distributed generation: A definition," *Electric Power System Research*, vol. 57, pp. 195-204, April 2001.

[3] M. Marie, E. El-Saadany, and M. Salama, "Flexible distributed generation: (FDG)," in *IEEE Power Engineering Society Summer Meeting*, 2002, vol. 1, pp. 49-53.

[4] C. Marnay and G. Venkatarmanan, "Microgrids in the evolving electricity generation and delivery infrastructure," in *IEEE Power Engineering Society General Meeting* 2006, pp. 1-5.

[5] E. Gumerman, R. Bharvirkar, K. LaCommare, and C. Marnay, "Evaluation framework and tools for distributed energy resources," Lawrence Berkeley National Laboratory, LBNL-52079, February 2003.

[6] R. Lasseter and P. Piagi, "Microgrid: A conceptual solution," in *Proceedings of the 35th IEEE Power Electronics Specialist Conference*, Germany, 2004, pp. 4285-4290.

[7] R. Lasseter and P. Piagi, "Extended microgrid using (DER) distributed energy resources," in *IEEE Power Engineering Society General Meeting*, 2007, pp. 1-5.

[8] R. Dugan, M. McGranaghan, S. Santoso, and H. Beaty, *Electrical Power System Quality*, 2nd ed. New York, NY: McGraw-Hill, 2003.

[9] W. Kuehn, "Control and stability of power inverters feeding renewable power to weak ac grids with no or low mechanical inertia," in *IEEE/PES Power Systems Conference and Exposition*, 2009, pp. 1-8.

[10] D. Klapp and H. Vollkommer, "Application of an intelligent static switch to the point of common coupling to satisfy IEEE 1547 compliance," in *IEEE Power Engineering Society General Meeting*, 2007, pp. 1-4.

[11] C. Marnay and O. Bailey, "The CERTS microgrid and the future of the macrogrid," Lawrence Berkeley National Laboratory, LBNL-55281, August 2004.

[12] P. Piagi and R. Lasseter, "Autonomous control of microgrids," in *IEEE Power Engineering Society General Meeting*, 2006, pp. 8-15.

[13] D. Feng and Z. Chen, "System control of power electronics interfaced distributed generation units," in *CES/IEEE 5th International Power Electronics and Motion Control Conference*, 2006, vol. 1, pp. 1-6.

[14] J. Liang, T. Green, G. Weiss, and Q. Zhong, "Hybrid control of multiple inverter in an island-mode distribution system," in *IEEE 34th Annual Power Electronics Specialist Conference*, 2003, vol. 1, pp. 61-66.

[15] T. Loix, K. De Brabandere, J. Driesen, and R. Belmans, "A three-phase voltage and frequency droop control scheme for parallel inverters," in *33rd Annual Conference of the IEEE Industrial Electronics Society*, 2007, pp. 1662-1667.

[16] C. Sao and P. Lehn, "Control and power management of converter fed microgrids," *IEEE Transactions on Power Systems*, vol. 23, no. 3, pp. 1088-1098, August 2008.

[17] P. Karlsson, J. Bjornstedt, and M. Strom, "Stability of voltage and frequency control in distributed generation based on parallel-connected converters feeding constant power loads," in *European Conference on Power Electronics and Applications*, 2005, pp. 10-19.

[18] M. Chandorkar, D. Divan and R. Adapa, "Control of parallel connected inverters in standalone ac supply systems," *IEEE Transactions on Industry Applications*, vol. 29, no. 1, pp. 136-143, January/February 1993.

[19] M. Illindala and G. Venkataramanan, "Control of distributed generation systems to mitigate load and line imbalances," in *IEEE 33rd Annual Power Electronics Specialists Conference*, 2002, vol. 4, pp. 2013-2018.

[20] G. Venkataramanan and M. Illindala, "Small signal dynamics of inverter interfaced distributed generation in a chain-microgrid," in *IEEE Power Engineering Society General Meeting*, 2007, pp.1-6.

[21] K. de Brabandere, B. Bolsens, J. Van den Keybus, J. Driesen, M. Rodanovic, and R. Belmans, "Small-signal stability of grid with distributed low-inertia generators taking into account line phasor dynamics," in *18th International Conference on Electricity Distribution (CIRED)*, Italy, 2005, pp. 1-5.

[22] M. Chandorkar, D. Divan, Y. Hu, and B. Barerjee, "Novel architectures and control for distributed UPS systems," in *9th Annual Conference Proceedings Applied Power Electronics Conference and Exposition*, 1994, vol. 2, pp. 683-689.

[23] J. Guerrero, J. Vasquez, J. Matas, M. Castilla, and L. de Vicuna, "Control strategy for flexible microgrid based on parallel line-interactive UPS systems," *IEEE Transactions on Industrial Electronics*, vol. 56, no. 3, pp. 726-736, March 2009

[24] A. Engler and N. Soultanis, "Droop control in LV-grids," in *2005 International Conference on Future Power Systems*, 2005, pp. 6-11.

[25] K. De Brabandere, B. Bolsens, J. van den Keybus, A. Woyte, J. Driesen, and R. Belmans, "A voltage and frequency droop control method for parallel inverters," *IEEE Transactions on Power Electronics*, vol. 22, no. 4, pp. 1107-1115, July 2007.

[26] J. Guerrero, J. Matas, L. de Vicuna, M. Castilla, and J. Miret, "Decentralized control for parallel operation of distributed generation inverters using resistive output impedance," *IEEE Transactions on Industrial Electronics*, vol. 54, no. 2, pp. 994-1004, April 2007.

[27] A. Bergen and V. Vittal, *Power Systems Analysis*, 2nd ed. Upper Saddle River, NJ: Prentice Hall, 2000.

[28] P. Sauer and M. Pai, *Power Systems Dynamics and Stability*. Englewood Cliffs, NJ: Prentice Hall, 1998.

[29] A. Fitzgerald, C. Kingsly, Jr., and S. Umans, *Electric Machinery*, 6th ed. New York, NY: McGraw-Hill Higher Education, 2003.

[30] R. Lasseter, "CERTS microgrid," in *IEEE International Conference on System of Systems Engineering*, 2007, pp. 1-5.

[31] J. Stevens, H. Vollkommer, and D. Klapp, "CERTS microgrid system tests," in *IEEE Power Engineering Society General Meeting*, 2007, pp. 1-4.

[32] J. Eto, R. Lasseter, B. Schenkman, J. Stevens, D. Klapp, H. Volkommer, E. Linton, H. Hurtado, and J. Roy, "Overview of the CERTS microgrid laboratory test bed," in *CIGRE/IEEE Power Engineering Society Joint Symposium Integration of Wide-Scale Renewable Resources Into the Power Delivery System*, 2009, pp. 1-8.

APPENDIX A – EQUIPMENT NAMEPLATE INFORMATION

Generator – Hampden Engineering Corporation

Model: Syn-2

Arm. Volts: 133/230 Arm. Amps: 15.5/9

Hp: 2 Ph: 3 Hz: 60 rpm: 1200

Frame: 215 Ser. Fac.: 1.15

Type: A000 Duty: Cont. Ins Class: F

Induction Motor – Teco Westinghouse Motor Corporation

Type: ASHEUW

Volts: 230/460 Amps: 5.21/2.6

Output: 2 hp 1.5kW Frame: 1457 Ins: F

Hz: 60 Ph: 3 rpm: 3450

Design: B NEMA Nominal Efficiency: 84.0

Kollmergen Holdline Brushless P.M. Servomotor

Stall Continuous: 10.3 rms amps 6.44 Nm

Stall Peak: 33.0 rms amps 19.5 Nm

Volts: 230 V rated rms L/L

Max Speed: 4900 rpm

APPENDIX B – EXPERIMENTAL DATA

B.1 System Data with No Droop

Speed	Generator 3	Generator 4	Generator 7	Generator 9
1198	18	21	5.5	9
1198	207	68	156	177
1198	424	331	385	393
1198	586	569	605	619
1198	658	606	615	630
1198	688	635	608	664
1198	719	649	648	687
1198	727	645	676	705
1198	742	685	688	721

B.2 System Data with Droop Gain k_p = 0.03

Speed	Generator 3	Generator 4	Generator 7	Generator 9
1214	217	198	156	153
1212	260	244	195	215
1212	319	287	250	245
1210	367	351	305	306
1208	418	399	354	352
1206	471	440	407	393
1206	522	494	445	446
1204	571	535	493	489
1202	563	568	512	528
1202	606	589	543	560
1200	643	610	562	578
1200	670	637	583	614
1200	690	657	617	628
1198	714	676	632	651
1198	730	695	650	671
1198	748	706	664	694
1196	766	737	693	697
1196	777	747	709	716
1196	798	748	630	595
1198	738	712	685	706

B.3 System Data with Load Increase Shown in Figure 19

Time (sec)	Speed (rpm)		Time (sec)	Speed (rpm)		Time (sec)	Speed (rpm)
345.19	1203		363.16	1202		381.13	1204
345.82	1195		363.77	1192		381.76	1202
346.43	1206		364.40	1199		382.37	1194
347.05	1203		365.02	1200		382.99	1195
347.66	1165		365.63	1202		383.62	1198
348.29	1231		366.26	1199		384.24	1198
348.90	1183		366.88	1192		384.85	1203
349.52	1203		367.51	1206		385.48	1200
350.13	1200		368.12	1203		386.08	1199
350.76	1202		368.74	1205		386.71	1201
351.38	1197		369.37	1203		387.33	1204
351.99	1196		369.98	1202		387.96	1197
352.62	1215		370.60	1200		388.57	1200
353.24	1206		371.23	1200		389.19	1205
353.85	1203		371.83	1197		389.82	1202
354.48	1189		372.46	1195		390.44	1204
355.10	1198		373.08	1197		391.05	1197
355.73	1196		373.71	1198		391.68	1199
356.34	1196		374.33	1205		392.29	1202
356.96	1189		374.94	1206		392.91	1202
357.59	1197		375.57	1191		393.54	1197
358.19	1195		376.18	1192		394.15	1195
358.82	1197		376.80	1203		394.77	1198
359.44	1204		377.43	1205		395.38	1205
360.07	1206		378.05	1198		396.01	1195
360.68	1201		378.66	1199		396.62	1206
361.30	1193		379.27	1203		397.24	1205
361.91	1199		379.90	1200		397.87	1203
362.54	1203		380.51	1197		398.47	1199